

Reduction of Cd²⁺/Ag⁺-induced toxicity by 3-mercaptopropionic acid-CdSe/ZnS quantum dots and glutathione-CdSe/ZnS quantum dots in human liver cancer cells

Jian Yin^{a,b,†,*}, Jie Zhang^{b,c,†}, Mingli Chen^{a,b}, Huancai Yin^{a,b}, Jingjing Tian^{a,b}

^a Department of Bio-Medical Diagnostics, Jinan Guo Ke Medical Technology Development Co., Ltd, Jinan, Shandong 250100 China

^b CAS Key Lab of Bio-Medical Diagnostics, Suzhou Institute of Biomedical Engineering and Technology, Chinese Academy of Sciences, Suzhou, Jiangsu 215163 China

^c School of Life Sciences, Shanghai University, Shanghai 200433 China

*Corresponding author, e-mail: yinj@sibet.ac.cn

† These authors contributed equally to this work and should be considered as co-first authors.

Received 11 Jun 2021, Accepted 14 Feb 2022
Available online 15 Apr 2022

ABSTRACT: In the present study, we investigated the interactions between CdSe/ZnS core/shell quantum dots (QDs) and Cd²⁺ and Ag⁺ in HepG2 cells. Two typical QDs, 3-mercaptopropionic acid-CdSe/ZnS QDs (QD-MPA) and glutathione-CdSe/ZnS QDs (QD-GSH) were applied and proved to be stable, as no fluorescence changes and Cd²⁺ releasing were detected during 24-h incubation. Both QDs tended to accumulate in HepG2 cells, and significantly reduced the harmful effects of Cd²⁺ and Ag⁺. Correspondingly, the intracellular and extracellular concentrations of free metal ions decreased by 2–5 folds due to their adsorption on QDs. On the other hand, both QDs exhibited no significant adsorption on cell fragments, suggesting that they accumulated inside cells but not on the membrane. Therefore, they did not hinder the uptake of free Cd²⁺ or Ag⁺. After all, the results revealed that highly stable QDs could extensively reduce the toxicity of heavy metals by absorption of heavy metal ions.

KEYWORDS: 3-mercaptopropionic acid-CdSe/ZnS quantum dots, glutathione-CdSe/ZnS quantum dots, Cd²⁺, Ag⁺, human hepatocellular carcinoma cells

INTRODUCTION

Nowadays, environmental exposure of quantum dots (QDs) are attracting more and more attentions, due to their wide application in industry and biomedical investigations [1–3]. Although QDs with inorganic shells (e.g., ZnS and CdS) and organic coatings (e.g., polyethylene glycol) were generally stable and safe [4], they could easily affect the transfer and toxicity of other pollutants, due to their large surface area and high reactivity [5]. Therefore, it is necessary to illustrate the potential interactions between QDs and other pollutants.

Although limited, but there are increasing reports on the potential interactions between QDs and trace metals in aquatic organisms and bacteria, since they are increasingly found to co-exist in the waste streams from laboratories and industries that synthesize or use them together [6]. It has been found that TGA-CdTe QDs enhanced the accumulation and toxicity of Cu²⁺ in zebrafish embryos and larvae, which might be due to the fact that Cu²⁺ was adsorbed onto QDs and entered zebrafish together [7]. With a similar mechanism, carboxyl-CdTe/CdS QDs also increased the uptake of Cu²⁺ and Pb²⁺ in metal-resistant bacteria *Cupriavidus metallidurans* [8]. An opposite result was reported by Worms et al [9], who found that carboxyl-CdSe/ZnS

QDs decreased the concentrations of lead and copper in the river, thus reducing the bioavailability and toxicity of metal ions to green microalgae. It seemed that the outcomes of QDs-metal mixtures should be dependent on the models used. However, such investigations have been seldom conducted in humans or animals, which should be more relevant and might occur due to workplace exposure or the accumulation through food chain [10].

This paper aimed to investigate the potential interactions between CdSe/ZnS QDs and Cd²⁺/Ag⁺ in human hepatocellular carcinoma (HepG2) cells. Two commercial QDs, 3-Mercaptopropionic acid-CdSe/ZnS QD (QD-MPA) and glutathione-CdSe/ZnS QD (QD-GSH), were applied. To clarify the relating mechanism, the stability of QDs and the adsorption ability of QDs on metal ions and cell membranes were respectively evaluated. The HepG2 cells were selected for the experiment because most of QDs tended to accumulate in the liver of treated animals [11]. Cd²⁺ and Ag⁺ were selected as they were increasingly released from anthropogenic activities, and were often used together with QDs [5, 12]. Meanwhile, ZnS coated CdSe QDs were often used for their low toxicity, high stability, and high fluorescence efficiency [13]. The reasons for using two different QDs, QD-MPA and QD-GSH, were to confirm our conclusions and to test the effects

of surface modifications, which was considered as a critical factor for the biological behavior of QDs [14].

MATERIALS AND METHODS

Cell line and reagents

HepG2 cells (ATCC HB8065) were purchased from Shanghai Cell Bank, Chinese Academy of Sciences (Shanghai, China). QD-MPA and QD-GSH were from Suzhou Xingshuo Nano Technology Co., Ltd (Suzhou, China). CdCl₂ and methyl thiazolyl tetrazolium (MTT) were obtained from Sigma-Aldrich (St Louis, MO, USA). Fetal bovine serum was from Sijiqing Biological Eng. Material Co. Ltd (Hangzhou, China). High glucose-Dulbecco's modified eagle medium (DMEM, containing 25 mM glucose, 4.0 mM L-glutamine, and no sodium pyruvate) was provided by Gibco (Gaithersburg, USA). AgNO₃ was obtained from Sinopharm Chemical Reagent Co., Ltd (Shanghai, China). Bicinchoninic acid protein assay kit was from Biyuntian Biotechnology Institute (Haimen, Jiangsu, China). Ultrapure water was produced by a Milli-Q Water System and used through the experiments (Millipore Corp., Bedford, MA, USA). The other chemicals were all of reagent grades and obtained from commercial suppliers.

QD Characterization

Stock solutions of QDs (10 mM) in distilled water were maintained at 4°C in the dark and consumed within 2 months. The shapes and diameters of QDs in distilled water (100 nM) were determined with a Tecnai G220 transmission electron microscope (TEM) (FEI, Portland, USA) operating at 200 kV. Photograph was taken by placing a drop of QD dispersion onto a copper mesh-supported carbon film. After dilution to 100 nM in DMEM medium, characteristics of QDs were detected. Emission spectra of QDs were obtained with a Hitachi F-4600 fluorescence spectrophotometer (Hitachi Co. Ltd, Tokyo, Japan) at an excitation wavelength of 370 nm. Dynamic light scattering and zeta-potential detections were performed with a Malvern Zetasizer Nano ZS90 equipment (Worcestershire, UK).

Cell culture and treatment

Stocks of QDs were diluted in DMEM medium before use. The maximum concentration of QDs was limited to 100 nM so that their final concentrations in distilled water would not exceed 1%, which significantly altered the osmotic pressure of culture medium. CdCl₂ and AgNO₃ were dissolved in DMEM medium directly.

HepG2 cells (15–25 passages) were seeded into 24-well plates at a density of 5×10^4 cells/well. Cells were cultured in 1 ml DMEM medium supplemented with 10% fetal bovine serum and 1% streptomycin/penicillin. The plates were maintained at 37°C in a humidified atmosphere with 5% CO₂. After reaching 80% of confluence, cells were washed with phos-

phate buffer saline (PBS) and treated with 1 ml DMEM medium containing QDs (10, 25, 50, and 100 nM), CdCl₂ (20, 40, 60, 80, 100, and 160 μM), AgNO₃ (10, 15, 20, 30, and 40 μM), or QDs (12.5, 25, 50, and 100 nM) + CdCl₂ (80 μM)/AgNO₃ (20 μM). After 24-h incubation, cells in each group were detected for their MTT values.

After reaching 80% of confluence, HepG2 cells in 24-well plates were washed with PBS and detected for the concentration- and time- dependent accumulations of QDs. For the effects of exposure concentrations, HepG2 cells were cultured in 1 ml DMEM medium containing different concentrations (25, 50, and 100 nM) of QD-MPA and QD-GSH. After 24-h treatment, cells were washed with ice-cold PBS and collected for accumulation experiments. For the effects of exposure time, we used 50 nM, the middle concentration, in the experiment. Cells were washed with PBS and cultured in DMEM medium containing. At 0.1, 0.5, 1, 3, 6, 12, and 24 h, cells were washed with ice-cold PBS and collected for accumulation experiments.

MTT reduction assay

The percentage of living cells in each group was detected with MTT assay [15]. In brief, cells were washed with PBS and incubated in 500 μl MTT solution (1 g/l dissolved in PBS) for 3 h at 37°C. After that, formazan crystals in each well were dissolved in 1.5 ml acidified-isopropanol at room temperature for 1 h. Absorbance of lysis at 490 nm was detected with a microplate reader (SynergyH1, Biotech, Winooski, VT, USA). Cell viability was calculated as the percentage of absorbance normalized to the control group.

QDs accumulation

After the treatment of QDs, cells in each well were washed with PBS, lysed in 0.5 ml 1% Triton-100 solutions (v/v, dissolved in PBS), and then centrifuged at 15 294g for 10 min to get rid of cellular fragments. The supernatant's fluorescence was detected with a microplate fluorescence reader (SynergyH1, Biotech, Winooski, VT, USA) with an ex/em wavelength of 485/590 nm. The amounts of QDs were quantified with a standard curve (0–50 pM). The values were normalized to the viable cell numbers ($MTT\% \times 2 \times 10^5$, nM/10⁵ cells) as described before [16]. 2×10^5 was the average numbers of cells reaching 80% confluence in 24-well plates as accessed by trypan blue exclusion methods.

Confocal laser scanning microscopy

Cellular accumulation of QDs were confirmed with confocal laser scanning microscopy. In brief, HepG2 cells were cultured on 35 mm glass bottom dish (well size 20 mm, cover gridded glass 0.13–0.16 mm, Cellvis, Mountain View, CA, USA) at a density of 1.5×10^5 cells/dish in 2 ml of DMEM medium supplemented

with 10% fetal bovine serum. After seeding for 4 h, the cells were washed with PBS and treated with DMEM medium containing 100 nM of QD-MPA or QD-GSH for 4 h, which caused no significant damages to the HepG2 cells. Subsequently, cells were fixed with 4% paraformaldehyde (m/v, dissolved in PBS) and observed with a Leica TCS SP5 II confocal microscope (Leica microsystems, Wetzlar, Germany) including a FITC filter and $\times 63$ oil immersion lens. Digital photographs were obtained by a Leica DFC350FX monochrome digital camera connected to the microscope.

Adsorption of metal ions onto QDs inside HepG2 cells

The intracellular concentrations of Cd^{2+} and Ag^+ were detected at first, to illustrate the reasons for the rescuing effects of QDs on the toxicity of metal ions. After reaching 80% of confluence, HepG2 cells in 24-well plates were exposed to 1 ml medium containing 80 μM CdCl_2 or 20 μM AgNO_3 with or without 100 nM QD-MPA/QD-GSH. After 24-h treatment, the cells were washed with ice-cold PBS, detached by trypsin-EDTA solution, and transferred to tubes containing 500 μl PBS. Intracellular concentrations of Cd^{2+} were measured with Leadmium™ Green AM assay kits (Thermo fisher Scientific, Inc., Waltham, MA, USA) following the manufactures' instructions. In brief, 4 μl Green AM dyes were added to each tube and incubated for 30 min in a 37 °C light-proof water bath. After that, the excess dyes were washed away by 0.85% NaCl. Finally, HepG2 cells were analyzed with a fluoLSR Fortessa flow cytometry (BD Biosciences, San Jose, CA, USA) using an excitation wavelength of 488 nm. For Ag^+ , the cells were lysed by sonication (40 kHz, 900 W, twice, 5 s) and centrifuged at 15 294g for 10 min to get rid of cellular fragments. The concentration of Ag^+ in the suspension was quantified using atomic absorption spectrometry (AA240FS-GTA120; Varian Inc., Palo Alto, CA, USA). In another experiment, HepG2 cells received the same treatment were analyzed by MTT assay. The obtained concentrations of $\text{Cd}^{2+}/\text{Ag}^+$ were divided by the viable cell numbers ($\text{MTT}\% \times 2 \times 10^5$, nM/ 10^5 cells), and normalized to the groups treated by $\text{Cd}^{2+}/\text{Ag}^+$ alone.

Adsorption of metal ions onto QDs in the culture medium

Further experiments were conducted to detect the adsorption of metal ions onto QDs in the culture medium, which would hinder the entry of QDs into cells by lowering extracellular concentrations of $\text{Cd}^{2+}/\text{Ag}^+$. In brief, 1 ml DMEM medium containing 80 μM CdCl_2 or 20 μM AgNO_3 with or without 100 nM QD-MPA/QD-GSH was incubated at 37 °C in a humidified atmosphere with 5% CO_2 . After that, the mixture was centrifuged at 108 800g for 10 min. The concentra-

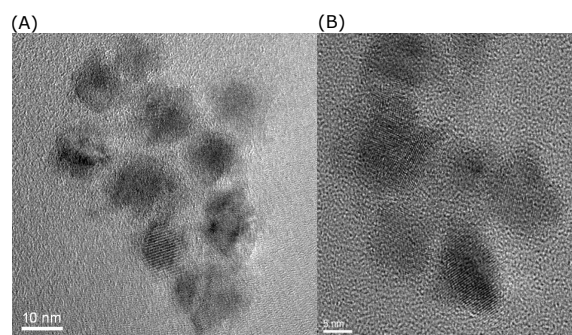


Fig. 1 Transmission electron microscopy images of QD-MPA (A) and QD-GSH (B), indicating the diameters of both QDs.

tions (in percentage) of free metal ions in the obtained supernatant were then detected with an AA240FS-GTA120 atomic absorption spectroscopy (Varian Inc., Palo Alto, CA, USA). The centrifugation speed was suggested by the manufactures and tested by our team, which could completely get rid of QDs and QD-metal complexes in the solutions.

Statistical analysis

All results were expressed as mean \pm SD of three independent experiments. One-way ANOVA test was applied to make comparisons between control and treatment groups. All analyses were conducted with SPSS Statistic 22.0 software (Chicago, Illinois, USA). p -value < 0.05 was considered significant.

RESULTS

Characterization of QDs

Using TEM detection, QD-MPA and QD-GSH were both found to be monodispersed in distilled water, and their diameters were 8.06 ± 0.98 nm and 8.28 ± 0.58 nm, respectively (Fig. 1). After dilution in DMEM medium, the characters of QDs were detected and summarized in Table 1. Among them, the zeta potentials of QD-MPA (-18.9 ± 0.5) and QD-GSH (-26.2 ± 1.1 mV) indicated that they were both negatively charged in the culture medium. The hydrodynamic radii of the QD-MPA and QD-GSH, which were 26.94 ± 1.21 nm and 16.14 ± 1.51 nm, respectively, indicated that they slightly aggregated in the DMEM medium. The maximum emission wavelength of QDs was 611 nm, corresponding to a red fluorescence. More importantly, the constant fluorescence intensity and negligible Cd^{2+} releasing indicated that both QDs did not change significantly during the 24-h culture (Fig. S1 and Fig. S2). Therefore, the toxicity of QDs and their interactions with metal ions should be caused by the QDs themselves.

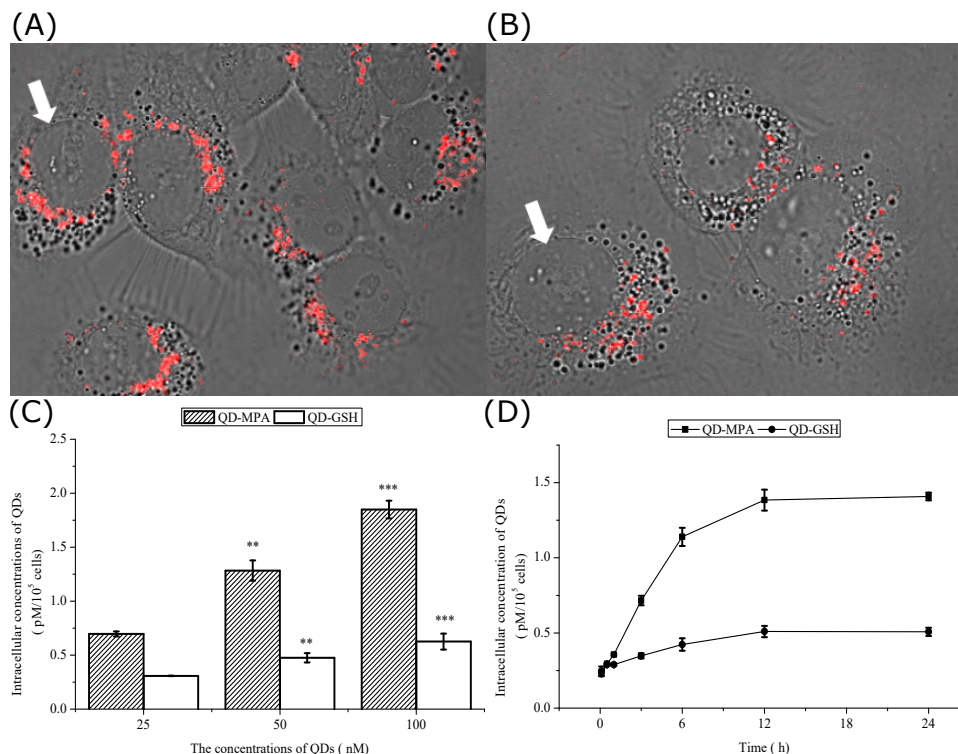


Fig. 2 Accumulations of QD-MPA (A) and QD-GSH (B) in HepG2 cells. Here showed merged photos of phase-contrast images and corresponding confocal fluorescence images. White arrow: Cell nucleus. Original magnification: × 630. Concentration- (C) and time- (D) dependent accumulations of QDs in HepG2 cells. Data represent mean values ± SD of three independent experiments with each in triplicates (*n* = 9). ** *p* < 0.01, *** *p* < 0.001 compared with groups treated with 25 nM QDs.

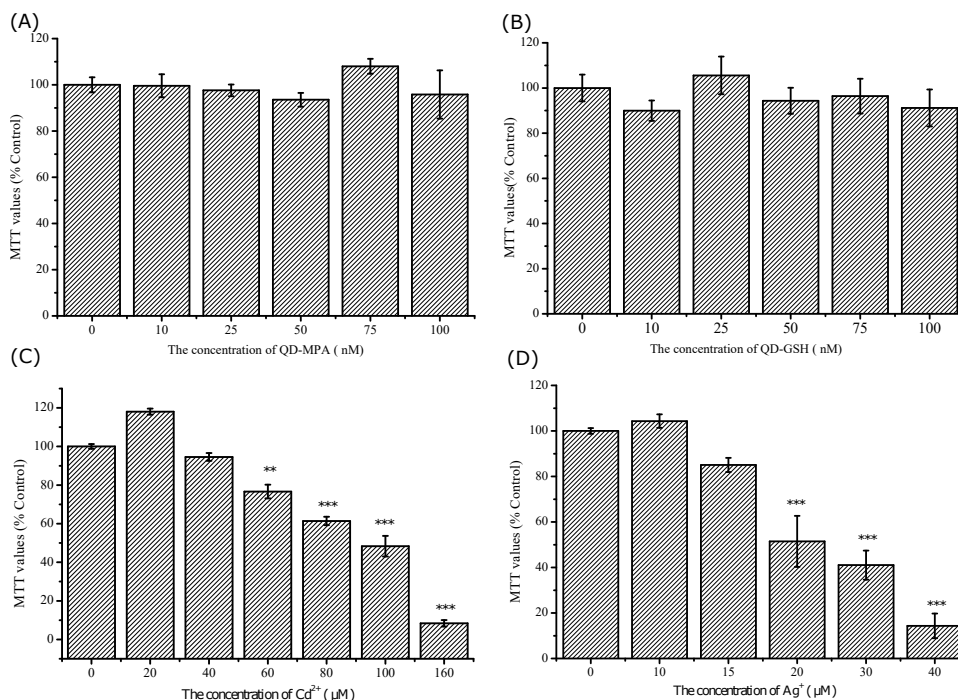


Fig. 3 Effects of QD-MPA (A), QD-GSH (B), Cd²⁺ (Cd, C) and Ag⁺ (Ag, D) on the proliferation of HepG2 cells. Data represent mean values ± SD of three independent experiments with each in triplicates (*n* = 9). ** *p* < 0.01, *** *p* < 0.001 compared with untreated control.

Table 1 The physicochemical properties of QD-MPA and QD-GSH.

QD	Diameter (nm)	Zeta-potential (mV)	Hydrodynamic diameter (nm)	Emission maximum (nm)
QD-MPA	8.06 ± 0.98	-18.9 ± 0.5	26.94 ± 1.21	611
QD-GSH	8.28 ± 0.58	-26.2 ± 1.1	16.14 ± 1.51	611

Cellular uptake of QDs

CdSe/ZnS QDs tended to accumulate extensively in the cytoplasm and close to the cell nucleus (Fig. 2A,B). In the following experiments, concentration- and time-dependent accumulations of QDs were evaluated.

During 24-h incubation, cellular accumulations of both QDs increased with the exposure concentrations (Fig. 2C). For example, with the treatments of 25 and 50 nM QD-MPA, the cellular accumulations of the QD were 2.05 ± 0.06 and 3.17 ± 0.09 nM per 10⁵ HepG2 cells, respectively, with a significantly higher accumulation caused by the 50 nM QD-MPA ($p < 0.001$). Similarly, cellular accumulation increased from 1.28 ± 0.09 to 4.66 ± 0.76 nM per 10⁵ cells after the treatment of 25–100 nM QD-GSH. In addition, the QD-MPA exhibited a higher cellular accumulation than the QD-GSH at the same concentrations. For instance, 100 nM QD-MPA caused a cellular accumulation of 7.84 ± 0.71 nM per 10⁵ cells in HepG2 cells, which was higher than that of 100 nM QD-GSH (4.66 ± 0.76 nM per 10⁵ cells).

At the same concentration of 50 nM, cellular uptakes of the two QDs were in a time-dependent manner (Fig. 2D). The 0.1–24 h accumulations of QD-MPA and QD-GSH were 0.23 ± 0.01–1.41 ± 0.03 pM per 10⁵ cells and 0.25 ± 0.04–0.51 ± 0.03 pM/10⁵ cells, respectively. The highest accumulation of both QDs occurred at 12 h, and no significant alterations occurred after then.

Individual toxicity of QDs and metal ions

After exposure to two QDs for 24 h, no obvious decreases in the values of MTT were noticed within the concentration range of 10–100 nM (Fig. 3A,B). Therefore, both QDs caused no significant changes of cell viability during the treatment. On the contrary, concentration-dependent toxicity was observed for both Cd²⁺ and Ag⁺ (Fig. 3C,D). Significant MTT reductions were found at the concentration of 60 μM for Cd²⁺ and at the 15 μM for Ag⁺. The median effective concentrations (EC₅₀) were around 80 μM for Cd²⁺ and 20 μM for Ag⁺, which were used in the following experiment.

Effects of QDs on the toxicity of metal ions

As shown in Fig. 4, toxicity of Cd²⁺/Ag⁺ could be attenuated by the addition of QD-MPA/QD-GSH, but in a different manner. For Cd²⁺, the rescuing effects of QD-MPA/QD-GSH were in a concentration-dependent manner (Fig. 4A,B). The MTT value of HepG2 cells af-

ter the exposure of 12.5 nM QD-MPA and 80 μM Cd²⁺ was 64.39 ± 2.46% of the control groups, which was significantly higher than that of the groups treated with 80 μM Cd²⁺ alone (47.86 ± 4.94%, $p < 0.01$). The values increased to 93.59 ± 0.90% after the treatment of 100 nM QD-MPA and 80 μM Cd²⁺. Similarly, exposure to 12.5–100 nM QD-GSH with 80 μM Cd²⁺ resulted in MTT values of 51.17 ± 2.09%–94.56 ± 2.36%. On the other hand, both QD-MPA and QD-GSH attenuated the toxicity caused by Ag⁺, but they did not show any variations among different concentrations (Fig. 4C,D).

Adsorption of Cd²⁺/Ag⁺ onto QDs

Since the toxicity of Cd²⁺ and Ag⁺ relied on their intracellular concentration, the effects of QD-MPA/QD-GSH on the accumulation of Cd²⁺/Ag⁺ in HepG2 cells were evaluated. Fig. 5A shows that the addition of 100 nM QD-MPA and QD-GSH reduced the contents of intracellular Cd²⁺, as compared with the CdCl₂-only treated groups, by 83.18% and 85.14%, respectively. Similarly, intracellular concentrations of Ag⁺ were reduced by the addition of 100 nM QD-MPA and QD-GSH to the extents of 45.18% and 70.47%, respectively (Fig. 5B).

Adsorption of Cd²⁺/Ag⁺ onto QDs could also occur in the culture medium, thus hindering the uptake of metal ions by cells. As shown in Fig. 5C, free Cd²⁺ in culture medium was extensively eliminated by 100 nM QD-MPA and QD-GSH to 11.53 ± 0.65% and 12.72 ± 1.06% of initial values, respectively; which were only slightly higher than the medium containing QD-MPA or QD-GSH alone (10.57 ± 0.61% and 10.78 ± 1.33%, Fig. 5C). Similarly, free Ag⁺ in the medium was reduced by 96.86% and 76.69% after the incubation with QD-MPA and QD-GSH for 24 h (Fig. 5D).

DISCUSSION

With the development of nanotechnology, more and more QDs were synthesized and released into the environment. The interaction between QDs and chemical pollutants is therefore inevitable [17]; especially, QDs have strong reaction capacity for other materials, due to their large specific surface area [18]. However, the investigation on the joint effects of QDs and heavy metals are still rare, particularly in human cells. Therefore, this paper aimed to evaluate the potential interactions between typical QDs, QD-MPA and QD-GSH, and heavy metals, Cd²⁺ and Ag⁺, in HepG2 cells. Further experiments were conducted to illustrate the inner mechanism of such interactions.

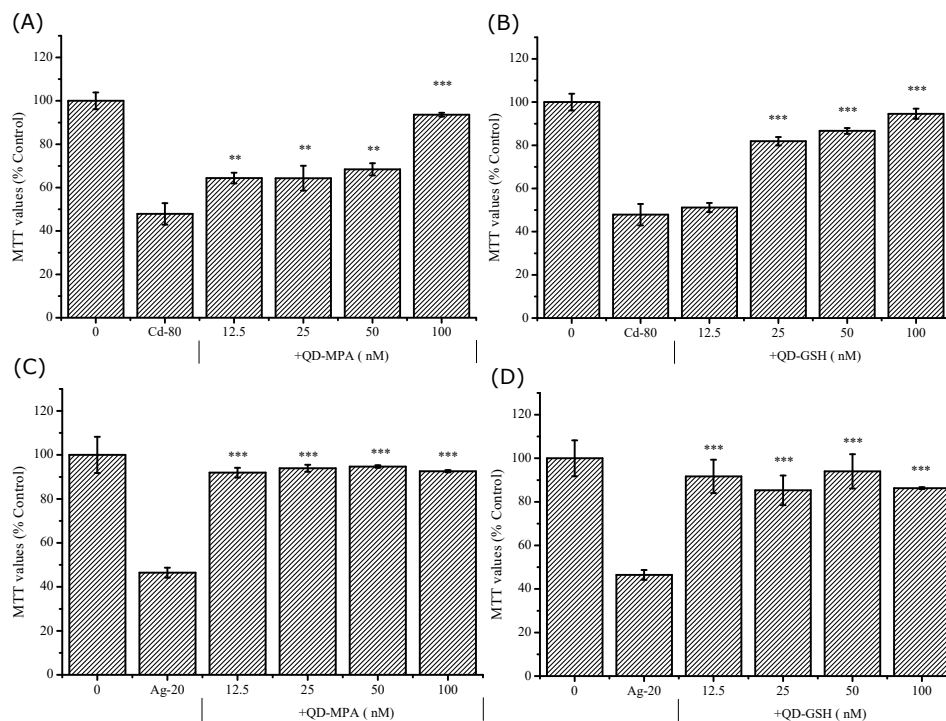


Fig. 4 Joint toxicity of: QD-MPA and Cd²⁺ (A); QD-GSH and Cd²⁺ (B); QD-MPA and Ag⁺ (C); and QD-GSH and Ag⁺ (D) in HepG2 cells. Data represent mean values ± SD of three independent experiments with each in triplicates (n = 9). ** p < 0.01, *** p < 0.001 compared with groups treated with Cd²⁺ or Ag⁺ alone.

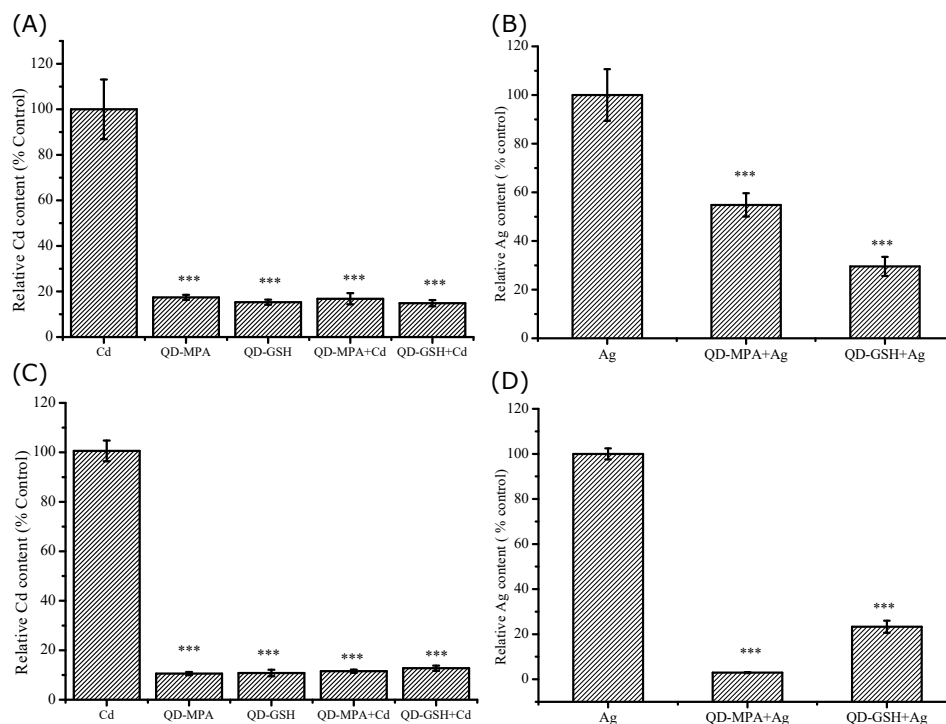


Fig. 5 Intracellular Cd²⁺ (A) and Ag⁺ (B) concentrations in HepG2 cells and extracellular Cd²⁺ (C) and Ag⁺ (D) concentrations after 24 h exposure to 80 μM Cd²⁺/20 μM Ag⁺ with or without 100 nM QD-MPA/QD-GSH. Data represent mean values ± SD of three independent experiments with each in triplicates (n = 9). *** p < 0.001 compared with groups treated by Cd²⁺ or Ag⁺ alone.

In the present study, treatment of both QD-MPA and QD-GSH exhibited a dose-dependent accumulation in HepG2 cells (Fig. 2) and without any obvious damages in the ranges of 10–100 nM (Fig. 3A,B). Compared with the extensively reported toxicity of CdTe and CdSe QDs [19–22], the core-shell structure significantly improved the biocompatibility and stability of QDs [23,24], which correlated well with our results. More importantly, the significant accumulations of both QDs in HepG2 cells (Fig. 2) indicated a possibility of reaction between the QD and the heavy metal ions absorbed by mammalian cells.

In general, the QD-GSH exhibited a low accumulation than the QD-MPA. This could be due to the slight larger hydrodynamic diameters and more negative potentials of QD-GSH in the culture medium (Table 1); smaller and less negative QDs could penetrate cell membranes more easily. Previous reports with HepG2 cells, monkey fibroblast-like cell lines, and mouse embryo fibroblasts found that gold nanoparticle (NP) toxicity was affected by the NP sizes, with smaller and more cationic nanoparticles exhibiting a higher accumulation [25,26], which correlated well with our results. In addition, Zhang et al [27] and Tian et al [28] found that multidrug-resistance associated proteins could pump out intracellular NPs in the form of GSH-conjugation in mouse hepatic cells and zebrafish embryos, which might be another reason for the decreased accumulation of QD-GSH.

Surprisingly, both QD-MPA and QD-GSH reduced the toxicity of Cd²⁺ and Ag⁺ in HepG2 cells in a large concentration ratio in 24 h (800:1 for Cd²⁺/QDs and 200:1 for Ag⁺/QDs, Fig. 4), which should be due to the fact that co-treatment of QD-MPA and QD-GSH with Cd²⁺/Ag⁺ extensively reduced the intracellular and the extracellular Cd²⁺/Ag⁺ concentrations used in experiment (Fig. 5). Due to electrostatic attraction effects, adsorption of positive metal ions onto negative NPs have been extensively reported for QDs, TiO₂, Ag, and SiO₂; but their intracellular fate were different depending on the stability of NP-Cd [5,29]. In this respect, if the complexes of Cd-QD or Ag-QD kept stable inside cells, the acute toxicity during 24-h treatment could be avoided. The reason for the higher efficiency of QDs adsorbing Cd²⁺/Ag⁺ should be due to the fact that it would be more difficult for QDs to after their binding to intracellular proteins like metallothionein [30].

In contrast to the accumulation rate, the QD-GSH exhibited more potent detoxification and adsorption effects on Cd²⁺/Ag⁺ than the QD-MPA. Such phenomenon could be firstly attributed to the more negative potential of QD-GSH, which was the main driving forces of QDs' adsorption of metal ions [31]. On the other hand, production of GSH in cells has been considered important in the elimination of ROS produced by Cd²⁺/Ag⁺ [32]. Therefore, GSH surrounding QD-

GSH could also be involved in this process.

Additionally, both QD-MPA and QD-GSH QDs adhered extensively to cationic liposomes, but exhibited negligible adsorption on the fragments of HepG2 cells (Fig. S3). Such phenomenon should be caused by the electrostatic attraction effects between the negatively charged QDs and the positively charged liposomes [33]. Meanwhile, the electrostatic repulsion between QDs and cell membranes caused no adsorption of the QDs onto the cell membranes. Therefore, the interactions between QDs and Cd²⁺/Ag⁺ should have mainly occurred in the cytoplasm of the HepG2 cells, where the QDs were located (Fig. 2).

It needs to be mentioned that, disruption of structures and releasing of core metals like Cd and Se are inevitable for metal-based QDs. Hence, the toxicity of Cd²⁺/Ag⁺ and QD-MPA/QD-GSH complexes could be expected in a longer time. However, our results revealed a possibility that NPs could reduce the accumulation and the toxicity of metal ions as long as the NP-metal complexes were stable, which could be an explanation for the decreased toxicity of metal ions by TiO₂ NPs in previous reports [34]. In addition, these results would be beneficial when applying safer NPs to eliminate heavy metal ions in the environment.

CONCLUSION

This study demonstrated for the first time that highly stable QDs could reduce the toxicity of Cd²⁺ and Ag⁺ towards HepG2 cells. The main reason for such phenomenon could be the adsorption of Cd²⁺ and Ag⁺ by QDs both inside and outside the cells. In-depth investigation on the controlling factors affecting the adsorption capability of QDs is strongly recommended. In addition, these results would be beneficial when applying safer nanoparticles such as Cd-free QDs to eliminate heavy metal ions in the environment.

Appendix A. Supplementary data

Supplementary data associated with this article can be found at <http://dx.doi.org/10.2306/scienceasia1513-1874.2022.070>.

Acknowledgements: This work was supported by grants from Natural Science Foundation of Shandong Province (No. ZR2019QB021), Shandong Province Key R&D Major Innovation Project (No. 2019JZZY011102), Primary Research & Development Plan of Jiangsu Province (No. BE2019673), Primary Research & Development Plan of Jiangsu Province (Grant BE2019051), and Primary Research & Development Plan of Jilin Province (Grant 20200403054SF).

REFERENCES

1. Wang HC, Bao Z, Tsai HY, Tang AC, Liu RS (2018) Perovskite quantum dots and their application in light-emitting diodes. *Small* 14, ID 1702433.
2. Fu Y, Gao G, Zhi J (2019) Electrochemical synthesis of multicolor fluorescent N-doped graphene quantum dots as a ferric ion sensor and their application in bioimaging. *J Mater Chem B* 7, 1494–1502.

3. Hana D, Yangb L, Hua Z, Dua Z, Wanga Y, Yuana Z, Wanga Q, Artemyevb M, et al (2020) Sharp fluorescence nanofiber network of CdSe/CdS core-shell nanoplatelets in polyvinylpyrrolidone. *ScienceAsia* **46**, 595–601.
4. Ulusoy M, Jonczyk R, Walter JG, Springer S, Lavrentieva A, Stahl F, Green M, Scheper T (2016) Aqueous synthesis of pegylated quantum dots with increased colloidal stability and reduced cytotoxicity. *Bioconjug Chem* **27**, 414–426.
5. Yu Z, Hao R, Zhang L, Zhu Y (2018) Effects of TiO₂, SiO₂, Ag and CdTe/CdS quantum dots nanoparticles on toxicity of cadmium towards *Chlamydomonas reinhardtii*. *Ecotoxicol Environ Saf* **156**, 75–86.
6. Shteplyuk I, Khranovskyy V, Yakimova R (2017) Insights into the origin of the excited transitions in graphene quantum dots interacting with heavy metals in different media. *Phys Chem Chem Phys* **19**, 30445–30463.
7. Zhang W, Miao Y, Lin K, Chen L, Dong Q, Huang C (2013) Toxic effects of copper ion in zebrafish in the joint presence of CdTe QDs. *Environ Pollut* **176**, 158–164.
8. Slaveykova VI, Pinheiro JP, Floriani M, Garcia M (2013) Interactions of core-shell quantum dots with metal resistant bacterium *Cupriavidus metallidurans*: consequences for Cu and Pb removal. *J Hazard Mater* **261**, 123–129.
9. Worms IA, Boltzman J, Garcia M, Slaveykova VI (2012) Cell-wall-dependent effect of carboxyl-CdSe/ZnS quantum dots on lead and copper availability to green microalgae. *Environ Pollut* **167**, 27–33.
10. Bouldin JL, Ingle TM, Sengupta A, Alexander R, Hannigan RE, Buchanan RA (2008) Aqueous toxicity and food chain transfer of quantum Dots (TM) in freshwater algae and *Ceriodaphnia dubia*. *Environ Toxicol Chem* **27**, 1958–1963.
11. Nurunnabi M, Khatun Z, Huh KM, Park SY, Lee DY, Cho KJ, Lee YK (2013) *In vivo* biodistribution and toxicology of carboxylated graphene quantum dots. *ACS Nano* **7**, 6858–6867.
12. Preeyanka N, Sarkar M (2021) Probing how various metal ions interact with the surface of QDs: implication of the interaction event on the photophysics of QDs. *Langmuir* **37**, 6995–7007.
13. Chakraborty D, Ethiraj KR, Chandrasekaran N, Mukherjee A (2021) Mitigating the toxic effects of CdSe quantum dots towards freshwater alga *Scenedesmus obliquus*: role of eco-corona. *Environ Pollut* **270**, ID 116049.
14. Alaghmandfard A, Sedighi O, Tabatabaei Rezaei N, Abedini AA, Malek Khachatourian A, Toprak MS, Seifalian A (2021) Recent advances in the modification of carbon-based quantum dots for biomedical applications. *Mater Sci Eng C Mater Biol Appl* **120**, ID 111756.
15. Yin J, Meng Q, Zhang G, Sun Y (2009) Differential methotrexate hepatotoxicity on rat hepatocytes in 2-D monolayer culture and 3-D gel entrapment culture. *Chem Biol Interact* **180**, 368–375.
16. Chen M, Yin H, Bai P, Miao P, Deng X, Xu Y, Hu J, Yin J (2016) ABC transporters affect the elimination and toxicity of CdTe quantum dots in liver and kidney cells. *Toxicol Appl Pharmacol* **303**, 11–20.
17. Mo D, Hu L, Zeng G, Chen G, Wan J, Yu Z, Huang Z, He K, et al (2017) Cadmium-containing quantum dots: properties, applications, and toxicity. *Appl Microbiol Biotechnol* **101**, 2713–2733.
18. Contreras EQ, Cho M, Zhu H, Puppala HL, Escalera G, Zhong W, Colvin VL (2013) Toxicity of quantum dots and cadmium salt to *Caenorhabditis elegans* after multigenerational exposure. *Environ Sci Technol* **47**, 1148–1154.
19. Gagne F, Auclair J, Turcotte P, Fournier M, Gagnon C, Sauve S, Blaise C (2008) Ecotoxicity of CdTe quantum dots to freshwater mussels: Impacts on immune system, oxidative stress and genotoxicity. *Aquat Toxicol* **86**, 333–340.
20. Tang S, Cai Q, Chibli H, Allagadda V, Nadeau JL, Mayer GD (2013) Cadmium sulfate and CdTe-quantum dots alter DNA repair in zebrafish (*Danio rerio*) liver cells. *Toxicol Appl Pharmacol* **272**, 443–452.
21. Zhang S, Jiang Y, Chen C-S, Creeley D, Schwehr KA, Quigg A, Chin W-C, Santschi PH (2013) Ameliorating effects of extracellular polymeric substances excreted by *Thalassiosira pseudonana* on algal toxicity of CdSe quantum dots. *Aquat Toxicol* **126**, 214–223.
22. Morelli E, Cioni P, Posarelli M, Gabellieri E (2012) Chemical stability of CdSe quantum dots in seawater and their effects on a marine microalga. *Aquat Toxicol* **122**, 153–162.
23. Sun H, Zhang F, Wei H, Yang B (2013) The effects of composition and surface chemistry on the toxicity of quantum dots. *J Mater Chem B* **1**, 6485–6494.
24. Modlitbova P, Porizka P, Novotny K, Drbohlavova J, Chamradova I, Farka Z, Zlamalova-Gargosova H, Romih T, et al (2018) Short-term assessment of cadmium toxicity and uptake from different types of Cd-based Quantum Dots in the model plant *Allium cepa* L. *Ecotoxicol Environ Saf* **153**, 23–31.
25. Coradeghini R, Gioria S, Garcia CP, Nativo P, Franchini F, Gilliland D, Ponti J, Rossi F (2013) Size-dependent toxicity and cell interaction mechanisms of gold nanoparticles on mouse fibroblasts. *Toxicol Lett* **217**, 205–216.
26. Ortega MT, Riviere JE, Choi K, Monteiro-Riviere NA (2017) Biocorona formation on gold nanoparticles modulates human proximal tubule kidney cell uptake, cytotoxicity and gene expression. *Toxicol In Vitro* **42**, 150–160.
27. Zhang Y, Hu Z, Ye M, Pan Y, Chen J, Luo Y, Zhang Y, He L, et al (2007) Effect of poly(ethylene glycol)-block-poly lactide nanoparticles on hepatic cells of mouse: low cytotoxicity, but efflux of the nanoparticles by ATP-binding cassette transporters. *Eur J Pharm Biopharm* **66**, 268–280.
28. Tian J, Hu J, Liu G, Yin H, Chen M, Miao P, Bai P, Yin J (2019) Altered gene expression of ABC transporters, nuclear receptors and oxidative stress signaling in zebrafish embryos exposed to CdTe quantum dots. *Environ Pollut* **244**, 588–599.
29. Dalai S, Pakrashi S, Bhuvaneshwari M, Iswarya V, Chandrasekaran N, Mukherjee A (2014) Toxic effect of Cr(VI) in presence of n-TiO₂ and n-Al₂O₃ particles towards freshwater microalgae. *Aquat Toxicol* **146**, 28–37.
30. Dong S, Shirzadeh M, Fan L, Laganowsky A, Russell DH (2020) Ag(+) ion binding to human metallothionein-2A is cooperative and domain specific. *Anal Chem* **92**, 8923–8932.
31. Willner MR, Vikesland PJ (2018) Nanomaterial enabled sensors for environmental contaminants. *J Nanobiotechnol* **16**, ID 95.
32. Hu J, Tian J, Zhang F, Wang H, Yin J (2019) Pxr- and Nrf2- mediated induction of ABC transporters by heavy

- metal ions in zebrafish embryos. *Environ Pollut* **255**, ID 113329.
33. Yang WW, Miao AJ, Yang LY (2012) Cd²⁺ Toxicity to a green alga *Chlamydomonas reinhardtii* as influenced by its adsorption on TiO₂ engineered nanoparticles. *PLoS One* **7**, e32300.
34. Ahamed M, Akhtar MJ, Alhadlaq HA (2019) Preventive effect of TiO₂ nanoparticles on heavy metal Pb-induced toxicity in human lung epithelial (A549) cells. *Toxicol In Vitro* **57**, 18–27.

Appendix A. Supplementary data

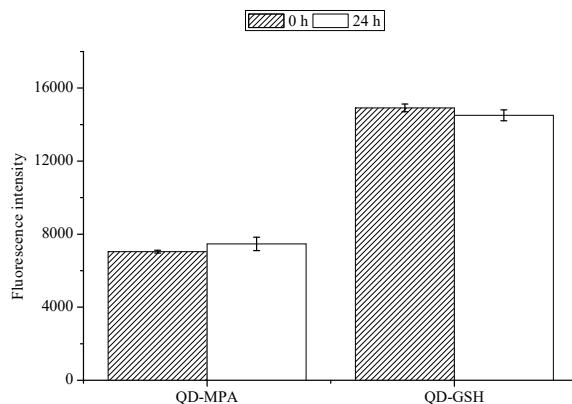


Fig. S1 Fluorescence intensity of QD-MPA/QD-GSH solutions when freshly-prepared (0 h) and at 24-h incubation in DMEM medium (24 h). Data represent mean values \pm SD of three independent experiments with each in triplicates ($n = 9$).

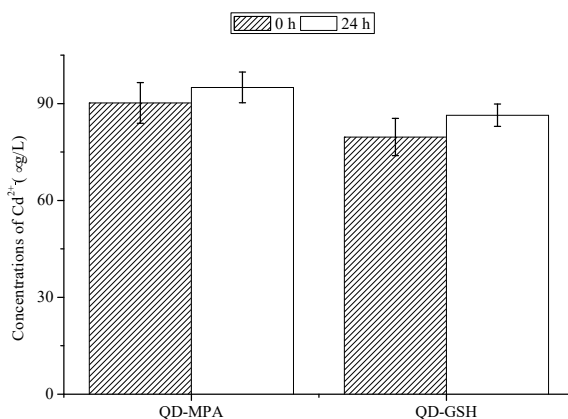


Fig. S2 Concentration of Cd²⁺ in QD-MPA/QD-GSH solutions when freshly-prepared (0 h) and at 24-h incubation in DMEM medium (24 h). Data represent mean values \pm SD of three independent experiments with each in triplicates ($n = 9$).

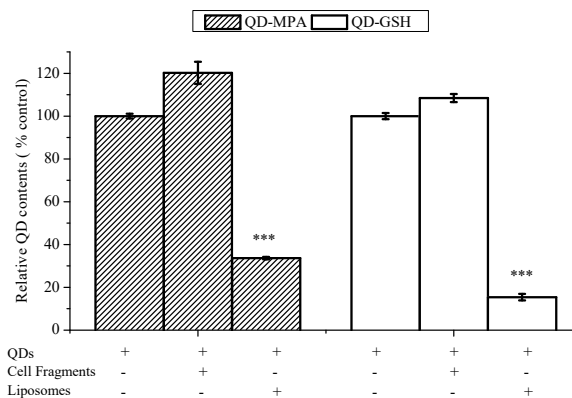


Fig. S3 Fluorescence intensity of 100 nM QDs after incubation at 37 °C for 24 h in the presence or absence of liposomes or cell fragments. Data represent mean values \pm SD of three independent experiments with each in triplicates ($n = 9$). *** $p < 0.001$ compared with groups treated by QD alone.